Sigma J Eng & Nat Sci 38 (3), 2020, 1623-1641

Sigma Journal of Engineering and Natural Sciences
Sigma Mühendislik ve Fen Bilimleri Dergisi

Research Article

A GENERAL OVERVIEW ON THE REGION-TIME BEHAVIORS OF THE RECENT EARTHQUAKE ACTIVITY IN THE MARMARA REGION OF TURKEY

Serkan ÖZTÜRK*[1], Serpil GERDAN[2]

[1]*Gümüşhane University, Department of Geophysics, GÜMÜŞHANE;* ORCID: 0000-0003-1322-5164
[2]*Kocaeli University, İzmit Vocational School, KOCAELI;* ORCID: 0000-0001-9126-7808

Received: 25.04.2020 Revised: 13.06.2020 Accepted: 25.07.2020

ABSTRACT

The principal aim of this study is to make a general assessment of the regional and temporal behaviors of the seismicity in the Marmara region of Turkey. For this purpose, the well-known spatio-temporal tools such as *Mc*-value, *b*-value, *Dc*-value, *Z*-value, recurrence period and annual probability were evaluated. The data catalog is homogeneous for local magnitude, M_L, and includes 18,662 events with $0.4 \leq M_L \leq 5.7$ between 2000 and 2020. Earthquake magnitudes change between 1.5 and 3.0 and hence, *Mc*-value was taken as 2.7. *b*-value was calculated as 1.14±0.07 and the earthquakes with small magnitude can be effective on this relatively large value. *Dc*-value was estimated as 1.57±0.03 with a scale invariance from 5.03 to 87.64 km. This moderate value means that distance between the epicenters approaches the diameter of cluster and, earthquake activity is more clustered in larger areas or at smaller scales. Time-magnitude estimations of annual probability and recurrence period indicate that the Marmara region has an intermediate/long terms hazard for the occurrence of strong/large earthquakes. Anomaly regions with low *b*-value and large *Z*-value observed at the beginning of 2019 can be considered as the most likely regions for strong/large earthquake occurrences in the next. As a remarkable fact, a correlation and combined interpretation of these seismotectonic parameters may supply a preliminary and essential perspective in the seismic hazard for strong/large earthquake occurrences in the Marmara region of Turkey in the intermediate/long terms.
Keywords: Marmara region, *Mc*-value, *b*-value, *Dc*-value, *Z*-value, seismic hazard.

1. INTRODUCTION

Spatio-temporal analyses of region-time-magnitude behaviors of seismicity for the seismic hazard and risk assessments have been carried out by different researchers for different parts of the world. Several researchers provided some remarkable results in the quantitative seismicity studies in recent years by using the well-known fundamental seismological tools such as (*i*) region-time-magnitude analysis of earthquake distribution, (*ii*) completeness magnitude, *Mc*-value, which defines the minimum magnitude of complete reporting, (*iii*) *b*-value, which is known as the power-law distribution of earthquake activity, (*iv*) *Dc*-value, which describes the self-similarity of a geometrical object, (*v*) standard normal deviate *Z*-value, which is one of the most

* Corresponding Author: e-mail: serkanozturk@gumushane.edu.tr, tel: (456) 233 10 00 / 5048

frequently used tool for the mapping of earthquake activity rate changes and (*vi*) recurrence times and annual probabilities for specific mag nitudes [1], [2], [3], [4], [5], [6], [7], [8], [9].

The basic and the best-known relationship of earthquake statistic is the Gutenberg-Richter (G-R) scaling law and this frequency-magnitude relation of earthquake distribution is given as *b*-value [10]. This power law distribution is preferred in the statistical seismology and seismic hazard assessments since it is crucial to forecast the occurrence of probabilities and recurrence times of the strong/large earthquakes. Region-time variations of *b*-value can be used to describe the behaviors of the seismotectonic environments, region-time-depth changes of stress and relative proportion of the small and large earthquakes [11]. Literature studies show that the *b*-value does not reflect only the relative proportion of the small and large earthquakes, but it can also be related to the features of the seismogenic environments, regional-temporal-depth changes of stress. In general, if there exists a temporal decrease in *b*-value for a given region, it can be commented that there may be a possibility of earthquake occurrence. Therefore, the G-R relationship is one of the best useful tools for earthquake statistic and many studies can be found for different parts of the world including Turkey [3], [12], [13], [14], [15].

Another basic characteristic of earthquake occurrences representing fractal properties is scale invariance or self-similarity. Systems or processes like seismicity has these features and can be represented by a power law distribution. Statistical studies show that earthquake behaviors have fractal and chaotic properties, and these properties are complex statistical tools in defining the earthquake distributions and its randomness [16]. The fractal feature is given by fractal dimension and the fractal dimension describes the heterogeneity of earthquake activity in the fault systems. Some geological, mechanical or structural variations in heterogeneity can be explained by using fractal dimension. Thus, fractal dimension of earthquakes, *Dc*-value, has widely been preferred as a useful parameter in recent years [4], [17], [18], [19], [20].

Besides the G-R relation and fractal dimension, region-time variations of the seismicity rate have also been used as the earthquake precursor. Precursory seismic quiescence, *Z*-value, is defined as a significant decrease in the average seismicity rate compared to the background activity [21]. This quiescence period can be observed in and around epicentral regions in several years before the main shock time, or this decrease may be separated from the main shock by a relatively short period with a tendency to increase in seismicity [22]. Investigation of earthquake activity rate changes is a significant process for the determining of seismic hazard since the quiescence period depends strongly on seismic and tectonic structures. The average duration of precursory quiescence before strong/large earthquakes in different parts of the world is given as 4.5±3 years [23]. There exist many studies on the analysis of precursory quiescence before main shock and these studies suggest that significant decrease in seismicity is observed in the epicentral area and its vicinity in a few years before the main shock [24], [25], [26], [27].

The North Anatolian Fault Zone (NAFZ) is one of the most critical tectonic units of Turkey with its clear fault trace and earthquake history. Therefore, this region was struck with many strong and devastating earthquakes in the past. The earthquake activity beginning with the large Erzincan earthquake in 1930 in the northeast of Turkey migrated to the western part of the NAFZ with the earthquake series in 1939, 1941, 1942, 1943, 1944, 1951, 1957, 1967, 1971 etc. Therewithal, two large and destructive earthquakes occurred in the Marmara part of the NAFZ at the previous century. The August 17, 1999 İzmit earthquake, *Mw*7.4, ruptured the NAFZ along the 145-km segment that extended from Gölyaka, Düzce, in the east, through the İzmit Bay into the Marmara Sea in the west, and the November 12, 1999, Düzce earthquake, *Mw*7.2, ruptured a part nearly 41-km long to the eastward [13]. These destructive earthquakes totally ruptured about the 1000-km segment of the NAFZ. In addition to these earthquakes, a strong earthquake (*Mw*5.8) occurred in the Marmara region in the recent year: September 26, 2019, Silivri-İstanbul (Marmara Sea) earthquake. Hence, the studies on revealing seismic hazard potential and earthquake prediction on the NAFZ have become very important. Therefore, the principal purpose of this study is to give some preliminary results for the seismic hazard by providing a region-time

analysis of seismotectonic parame ters for the Marmara region of Turkey at the beginning of 2020. For this purpose, a detailed statistical analysis of two basic size scaling parameters, the *b*-value of G-R relation and *Dc*-value of the fractal feature were achieved. Also, some estimations on completeness magnitude *Mc*-value, seismic quiescence *Z*-value, annual probability and recurrence time of the earthquakes for specific magnitude sizes were made in order to provide the current and next earthquake potential in this region.

2. MAIN SEISMOTECTONIC STRUCTURES AND EARTHQUAKE DATABASE

The NAFZ is known as one of the most seismically and tectonically active strike-slip faults in Turkey and the world. This fault zone forms a border to the east between the North Anatolia and the East Anatolia, and it shows a sub-parallel structure to the Black Sea coast. This transform fault zone extends for 1200 km from the Saros Gulf in the northern Aegean Sea to the Karlıova town in eastern Turkey and keeps a quite regular distance of some 100 km to the coast [28]. The dextral motion related to the NAFZ continues through the northern Aegean and crosses the northern central mainland Greece as a broad movement and eventually links up with the Hellenic subduction zone. The NAFZ has also some second order faults which splay from it into the Anatolian Plate. This zone shows strike-slip faulting with a reverse component in the east due to the constricting of the Arabian plate, whereas the western part exhibits a normal component owing to the interaction of the Aegean extensional regime. The NAFZ accommodates 24-30 mm/year of dextral displacement and its cumulative movement is estimated to vary from 40 km to a few hundred meters [29]. Active tectonics in Marmara part of the NAFZ can be summarized as the Düzce fault (DF), Eskişehir, İnönü-Dodurga and Kaymaz faults (EİDKF), Gemlik fault (GMF), İznik-Mekece fault (İMF), Geyve fault (GYF), Manyas fault (MSF), Yenice-Gönen and Sarıköy faults (YGSF), Etili fault (EF) and Saros-Gaziköy fault (SGF). Tectonic environments for the Marmara region were modified from different studies such as Bozkurt [28], Şaroğlu et al. [30] and given in Figure 1. Also, many details of the seismicity, local faults and tectonic structures for Marmara region can be found from several sources such as Demirtaş and Yılmaz [31], Emre at al. [32].

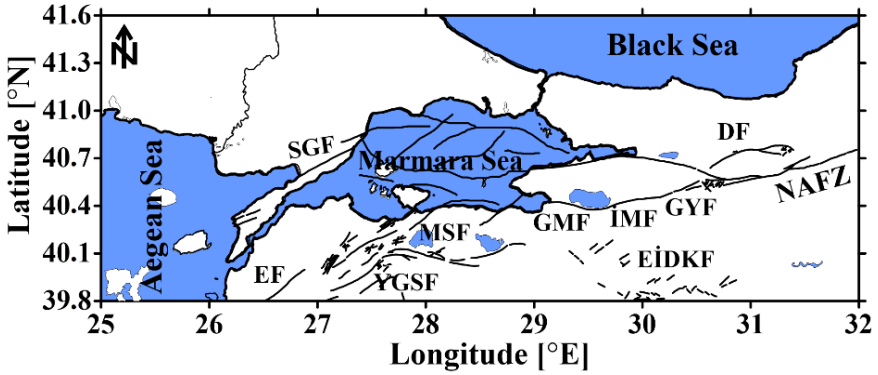

Figure 1. Main tectonic units in Marmara region (modified from Bozkurt [28] and Şaroğlu et al. [30]).

The NAFZ has experienced many large/destructive earthquakes during the past 60 years. The Karlıova section has ruptured during two successive earthquakes on August 19 (*Ms*6.8) and 20 (*Ms*6.2), 1966, respectively. December 26, 1939 Erzincan earthquake (*Ms* 7.9 to 8.0) is one of the largest earthquakes occurred in Turkey. This earthquake has an important role in triggering the other earthquakes of 1939-1967 sequences occurred in a westward progression: December 20,

1942 Erbaa-Niksar (*Ms*7.1), November 26, 1943 Tosya (*Ms*7.6), February 1, 1944 Bolu–Gerede (*Ms*7.3), August 13, 1951 Çankırı (*Ms*6.9), May 26, 1957 Abant (*Ms*7.0), July 22, 1967 Mudurnu valley (*Ms*7.1). In addition, the earthquakes recently occurred in the NAFZ can be given as March 13, 1992 Erzincan (*Ms*6.8), August 17, 1999 Izmit (*Ms*7.4), November 12, 1999 Duzce (*Ms*7.2), November 3, 2010 Saros Gulf (*Ms*5.3), June 7, 2012 Marmara Sea (*Ms*5.1), July 30, 2013 Gökçeada-Çanakkale (*Ms*5.3) and September 26, 2019 Silivri-İstanbul (*Ms*5.7) earthquakes [13], [28]. In the historical period (1800 BC-1900 AD), destructive earthquakes occurred in Marmara region, especially on the main segments of the NAFZ, in the intensity ranges of Io=IX-X. Epicenter distributions and dates of the historical earthquakes in Marmara region in the historical period were redrawn from the website of the Boğaziçi University, Kandilli Observatory and Research Institute (KOERI, URL-1) and plotted in Figure 2.

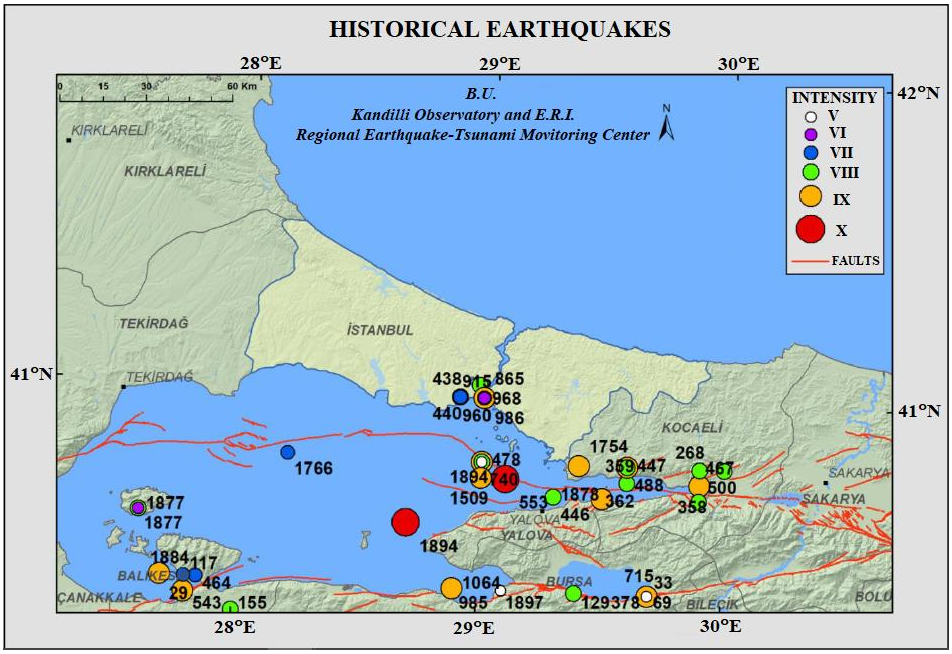

Figure 2. Epicenter distributions, dates and intensities of the historical earthquakes in Marmara region (modified from KOERI, URL-1).

Earthquake database used in this study was combined from the catalogs of Boğazici University, Kandilli Observatory and Research Institute (KOERI) and Disaster and Emergency Management Authority (AFAD) for the time period between 2000 and 2020. These institutions have high-gain seismometers and the errors of hypocenter distributions are given nearly 2 or 3 km depending on the distribution of stations. Each station, particularly after 2000, mostly supplies the type of M_d for all earthquakes. However, in recent years, they give the local magnitudes, M_L, of the earthquakes for unknown M_d. In the situations that M_d was not calculated in KOERI and AFAD catalogs between 2000 and 2020; unknown M_L values were computed from M_d-M_L equations provided by Kalafat [33]. For the statistical region-time evaluation, an original database including 18,662 shallow (depth<70 km) earthquakes from January 1, 2000 to January 21, 2020 with magnitude sizes between 0.4 and 5.7 was used. Earthquake database is homogenous for local magnitude, M_L, and time length of the catalog is nearly 20.06 years. Epicenter distributions of all 18,662 earthquakes were shown in Figure 3 with different symbols for different magnitude levels.

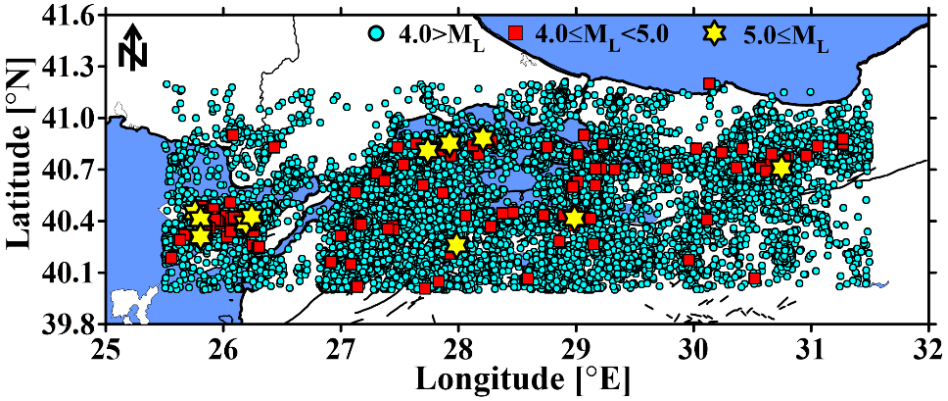

Figure 3. Epicenter distributions of 18,662 shallow earthquakes with $0.4 \leq M_L \leq 5.7$ between 2000 and 2020.

3. BRIEF DESCRIPTION OF THE ANALYSIS METHODS

Statistical behaviors of earthquake activity in Marmara region of Turkey were tried to describe with the best-known seismotectonic parameters such as *b*-value of magnitude-frequency distribution of earthquakes, *Dc*-value of the fractal feature of earthquake occurrences, standard normal deviate *Z*-value (called precursory seismic quiescence), completeness magnitude, annual probability and recurrence time of different magnitude levels. The assessment of these parameters was provided by discussing the region-time characteristics of seismicity at the beginning of 2020.

3.1. *b*-value of Gutenberg-Richter Relation, Annual Probability and Return Period

The basic relation of earthquake statistics in seismology was known as Gutenberg and Richter [10] power-law. This empirical relation defines the magnitude-frequency distribution of earthquake occurrences and is given as follow:

$$\log_{10} N(M) = a - bM \tag{1}$$

Where *N(M)* is the cumulative number of events during a particular time interval with magnitudes higher than or equal to *M*. The slope of the magnitude-frequency distribution gives *b*-value, whereas *a*-value shows the earthquake activity level. *a*-value exhibits significant changes from region to region and these variations depend on the length of the study area, time period of the catalog as well as the number of earthquakes. The *b*-value varies from 0.3 to 2.0 for different earthquake regions of the world [34], whereas an average of *b*-value in G-R relation is given as nearly 1.0 [35]. There are many factors affecting *b*-value changes. Although *b*-value is related to the relative numbers of small and large earthquakes, laboratory studies on rock fractures show that a decrease in *b*-value is associated with an increase in shear stress and a reduction in restricted compression. Furthermore, some factors such as thermal gradient, crack density, fault length, geological complexity, slip distribution, material properties and strain circumstances cause the variations in *b*-value [11], [36]. Thus, the *b*-value is scale-invariant and plays an important role in the earthquake prediction.

Annual probability of the earthquakes with different magnitude values and within any period can be calculated from the following equation [9]:

$$P(M) = 1 - e^{-N(M)*T} \tag{2}$$

where *P(M)* is the probability that at least one earthquake will occur in specific *T* years. *M* is taken from Equation 1. Return periods of the earthquakes with different magnitude levels can be computed from the following formula [9]:

$$Q = 1/N(M) \tag{3}$$

3.2. Fractal Features of Earthquake Occurrences (*Dc*-value)

The fractal dimension is a real number and measures the geometry of a distribution. Fractal distribution or correlation dimension implies that the number of events larger than a specified size has a power law dependence on the size. It shows spatial and temporal changes, hence, earthquake distributions are thought to be fractal, but not directly. The clustering properties of the spatial and temporal distributions of earthquakes can be analyzed by using the two-point correlation dimension. Fractal dimension, *Dc*, and the correlation sum, *C*(*r*), can be defined as follows [37]:

$$Dc = \lim_{r \to 0} \left[\log C(r) / \log r \right] \tag{4}$$

$$C(r) = 2N_{R<r} / N(N-1) \tag{5}$$

where *C*(*r*) is the correlation function, *r* is the distance between two epicenters and *N* is the number of earthquake pairs separated by a distance *R*<*r*. If the epicenter distribution has a fractal structure, the following equation can be given:

$$C(r) \sim r^{Dc} \tag{6}$$

where *Dc* is the fractal dimension or the correlation dimension. Distance *r* (in degrees) between two epicenters can be computed from the following equation:

$$r = \cos^{-1}\left(\cos\theta_i \cos\theta_j + \sin\theta_i \sin\theta_j \cos(\phi_i - \phi_j)\right) \tag{7}$$

where (θ_i, ϕ_i) and (θ_j, ϕ_j) are the latitudes and longitudes of the i^{th} and j^{th} earthquakes, respectively [13]. *Dc*-value can be obtained by fitting a straight line to a plot of *C*(*r*) versus *r* on a double logarithmic scale, practically from the slop of the graph. If *r* is small, the lack of points outside the cluster does not influence *C*(*r*). Therefore, *C(r)* will increase rapidly with *r* and large *Dc* can be expected. Besides, if a scaling range using low *r* is preferred to estimate *Dc*, robust clustering will fallow an increase in *Dc*. If *r* close to the diameter of the cluster, the rate at which *C(r)* increases with *r* reduces and *Dc* will be small. Thus, if a scaling range using large *r* values preferred to calculate *Dc*, robust clustering will cause a decrease in *r*. Depending on the size of *r* considered, this signifies that a dense cluster of points can give both large or small *Dc*-values [2].

Spatial and temporal fractal properties of earthquake distributions can be described with fractal dimension and therefore, earthquake distributions follow fractal statistics. The fractal dimension of earthquakes can be calculated for the estimation of possible unbroken sites mentioned as seismic gaps that may be broken in the next [2]. Therefore, the changes in fractal features mostly depend on the complexity or quantitative measure of the heterogeneity degree of seismicity in the fault systems. The larger *Dc*-value related to the smaller *b*-value is the dominant structural characteristic in the regions of increased complexity in the active fault systems. Also, these changes on the fractal dimension may be depended on the clusters of events and may be interpreted as an indication of stress changes on fault planes of the smaller surface area [2], [3].

3.3. *Z*-value of Standard Normal Deviate (Precursory Seismic Quiescence)

The phenomenon of precursory seismic quiescence was firstly proposed by Wyss and Habermann [38] and then Wiemer and Wyss [39] developed a methodology that can be applied in *ZMAP* software [40]. Some different techniques can be used to describe and to evaluate the seismic activity rate changes for different parts of the world. Most of them use spatial and temporal modeling of seismic quiescence before the main shocks. The standard normal deviate *Z*-test is one of the best known statistical methods frequently used for imaging the seismic quiescence regions. In order to rank the significance of precursory quiescence, the standard normal deviate *Z*-test can be used, generating the LTA (Long Term Average) function for the statistical evaluation of the confidence level in units of standard deviations [39]:

$$Z(t) = \frac{R_{all} - R_{wl}}{\left[\left(\sigma^2{}_{all} / n_{all}\right) + \left(\sigma^2{}_{wl} / n_{wl}\right)\right]^{1/2}} \tag{8}$$

where R_{all} is the mean seismicity rate in the overall foreground period, R_{wl} is the average number of earthquakes in the background window, σ and n are the standard deviations and the number of samples within and outside the window, respectively. *Z*-value estimated as a function of time is called as LTA.

3.4. Declustering Process of the Catalog and Completeness Magnitude (*Mc*-value)

Some dependent events such as foreshocks, aftershocks or swarms frequently affect the spatial and temporal statistics of earthquakes. For this reason, the separation of secondary events from the catalogs is a significant stage for reliable and high-quality seismic hazard analyses. Therefore, earthquake catalogs need to be declustered and earthquakes must be separated into primary and secondary events. At the end of this process, all dependent earthquakes can be separated from independent ones and these dependent events are substituted with a unique event by eliminating each cluster. In this study, the declustering technique based on the algorithm modeled by Reasenberg [41] was used in order to decluster (or decompose) the earthquake catalog through *ZMAP* software. Since this method has been widely used for different earthquake catalogs in the world, Reasenberg's declustering method was preferred.

Completeness magnitude, *Mc*-value, is a very significant parameter for the statistical seismicity studies. *Mc*-value is defined as the minimum magnitude of complete recording and can be estimated from the frequency-magnitude distribution of earthquakes [1]. This magnitude level contains 90% of the earthquakes in the catalog and temporal changes in *Mc*-value can affect the results of the statistical analyses, especially in *b* and *Z*-values [9]. Therefore, the maximum number of earthquakes in the catalog is aimed to be used for high-quality results for the analysis of all statistical parameters. G-R size scaling law against magnitude can be used to estimate *Mc*-value, and the changes in *Mc*-value can be estimated by using a moving time window approach [1]. Thus, the knowledge of temporal *Mc*-value is significant and the estimation of temporal *Mc*-value variations was achieved carefully as the first step in this study because *Mc*-value was used in the calculations of statistical parameters.

There are 18,662 earthquakes in the catalog with magnitudes $0.4 \leq M_L \leq 5.7$ between 2000 and 2020. After declustering process, 3755 events (approximately 20.12%) were eliminated and 14,907 earthquakes remained. For the original catalog including all shallow earthquakes with $M_L \geq 0.4$, *Mc*-value changes between 1.8 and 2.8 from 2000 to 2020 and hence, it was used as 2.7 on average (Figure 4). Since magnitude completeness analysis is quite effective on the correct estimation of *b*-value, *Z*-value, annual probability and recurrence time, temporal *Mc*-value was carefully analyzed and estimated. The number of earthquakes with magnitude $M_L < 2.7$ is 9587 and all earthquakes with magnitude $M_L < 2.7$ were removed from the catalog. Finally, after

declustering and separating M_L<2.7 events, nearly 71.49% of all earthquakes was eliminated and the number of earthquakes for seismic hazard analysis was reduced to 5320 (Figure 5). As a remarkable fact, a more reliable, homogeneous and robust earthquake catalog was obtained after these processes and this database was used as the final data catalog.

4. RESULTS AND DISCUSSIONS

In this study, a detailed spatio-temporal analysis of recent seismic activity for Marmara part of the NAFZ of Turkey was performed. For this purpose, the best known and the most frequently used seismotectonic parameters such as completeness magnitude, *Mc*-value, (ii) Gutenberg-Richter *b*-value, (iii) fractal dimension *Dc*-value, (iv) standard normal deviate *Z*-value, (v) annual probability and (vi) recurrence time of earthquake occurrences were evaluated. In order to describe the behaviors of earthquake occurrences, the region-time-magnitude variations of earthquakes were mapped at the beginning of 2020. All spatial and temporal analyses were performed with *ZMAP* software package. *b*-value was estimated with the maximum likelihood estimation since it provides a reliable estimate than that of the least-square regression method, whereas *Dc*-value was calculated by linear regression with 95% confidence limits since this is suggested as the most suitable method by the authors aforementioned.

Time changes of *Mc*-value are non-stable and hence, estimation of temporal *Mc*-value is the first and most significant step. The estimation of *Mc*-value as a function of time was realized by using a moving window technique. *Mc*-value was plotted with its standard deviation for every 175 earthquakes per window and the original database including 18,662 events with M_L≥0.4 was used. Time variations of *Mc*-value were shown in Figure 4. As shown in Figure 4, *Mc*-value is relatively large and changes between 2.6 and 2.8 from 2000 to 2012, whereas it generally varies from 2.0 to 2.6 between 2012 and 2013. Then, it changes between 2.2 and 2.0 from 2012 to 2017 while it decreases to about 1.8 at the beginning of 2020. It can clearly be observed that *Mc*-value is in and around 2.7 until 2012, whereas *Mc*-value shows a decreasing trend and it has an average value of 2.0 after 2013. KOERI and AFAD have provided real-time data with a great number of modern on-line and dial-up seismic stations in and around the study region in recent years and hence, the minimum level of recording magnitude shows decreases with time since the number of seismographs increases. *Mc*-value estimation is a significant step since this study includes *b*-value and *Z*-value statistics. From this point of view, an average *Mc*-value was assumed as 2.7, which represents well all the time intervals of the catalog. The cumulative number of the earthquake with time for the original catalog with M_L≥0.4 including 18,662 earthquakes, for the declustered catalog with M_L≥0.4 including 14,907 earthquakes and for the declustered catalog with M_L≥2.7 containing 5320 earthquakes was shown in Figure 5. As seen in Figure 5, cumulative number of declustered earthquakes with M_L≥2.7 has a smooth slope when compared to the original database. Some authors stated that magnitude completeness analysis and declustering of the catalog are critical in the description of the region-time earthquake behaviors [9], [26], [42], [43]. These studies indicate that dependent earthquakes such as foreshocks, aftershocks or swarms should be removed from the catalog before the analyses. As clearly seen from Figure 5, declustering process and removing M_L<2.7 earthquakes from the original database eliminated the dependent events. As a remarkable fact, after these two steps, more homogeneous and more robust earthquake data was obtained for the region-time analyses of statistical parameters.

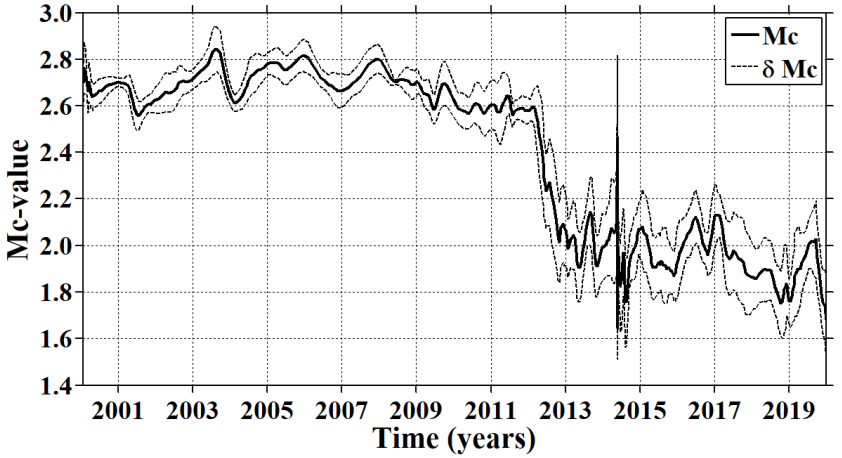

Figure 4. Time variations of *Mc*-value from 2000 to 2020, as well as itsstandard deviation (*δMc*).

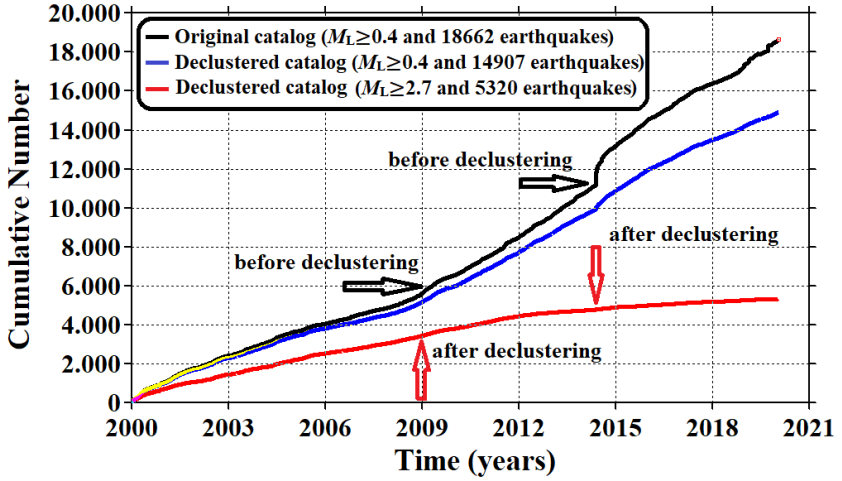

Figure 5. Cumulative number of earthquakes with time for the original data with $M_L \geq 0.4$, for the declustered catalog with $M_L \geq 0.4$ and for the declustered catalog with $M_L \geq 2.7$.

Figure 6 shows the magnitude and time histograms of the earthquakes in the Marmara region between 2000 and 2020. As stated in the data section, magnitudes of the events changes between 0.4 and 5.7, and earthquake numbers have an exponential decay rate from smaller to larger magnitudes. As seen in Figure 6a, the magnitudes of many earthquakes change between 1.5 and 3.5. Earthquake numbers show two maxima in M_L=2.1 and M_L=2.7 levels. The number of earthquakes with $1.5 \leq M_L < 3.5$ is 17,303, whereas there are 1359 events with $3.5 \leq M_L < 5.7$. Also, there are 915 events for $0.4 \leq M_L < 1.5$, 15,565 events for $1.5 \leq M_L < 3.0$, 2041 events for $3.0 \leq M_L < 4.0$, 200 events for $4.0 \leq M_d < 5.0$, and 11 events for $5.0 \leq M_L$. Thus, events with a magnitude between 1.5 and 3.5 occur more frequently than those of the others in Marmara and its surrounding area. This increasing trend in the number of small events may be an indication of stress accumulation in this region in recent years. The time histogram of the events from 2000 to 2020 was also demonstrated in Figure 6b. The seismicity from 2000 to May 24, 2014 shows some fluctuations and the number

of earthquakes for all magnitude levels in this time interval is 11,148. There are some increases in seismicity after 2009 although the number of earthquakes from 2014 to 2020 shows both strong increases and decreases. There are 5582 events between 2000 and 2009, and there are 5566 earthquakes between 2009 and May 24, 2014. However, a systematic decrease in earthquake activity after May 24, 2014 shows an increasing trend between 2019 and 2020, and the total number of events between these years is 1337. As a remarkable fact, these types of statistical analyses may supply the preliminary perspective for the analysis of seismicity rate changes and these evaluations can be related to the region-time changes of precursory seismicity in and around the Marmara region.

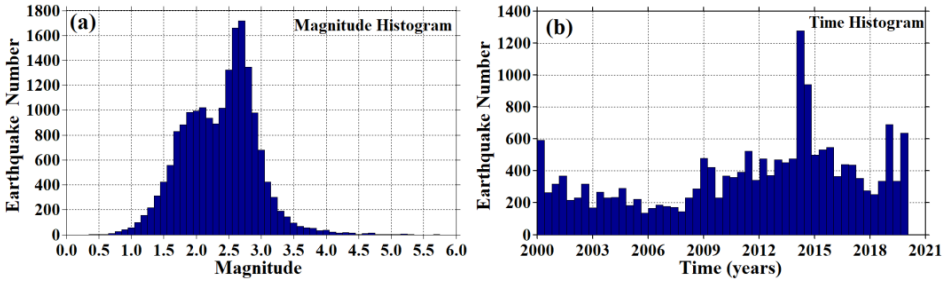

Figure 6. (a) Magnitude histogram and (b) Time histogram of the seismicity in Marmara region from 2000 to 2020.

Figure 7 shows the *b*-value of G-R frequency-magnitude distribution and fractal statistics of the seismicity in the Marmara region at the beginning of 2020. The *b*-value was estimated with the maximum likelihood method and shown in Figure 7a. As shown from the temporal changes of *Mc*-value, average *Mc*-value was taken as 2.7 for all the catalog including 18,662 earthquakes between 2000 and 2020, and the *b*-value was computed as 1.14±0.07. *b*-value, its standard deviation, *a*-value, and *Mc*-value were also shown in Figure 7a. As stated above, the *b*-value varies from 0.3 to 2.0 on a global scale [34] and tectonic earthquakes are known to have a *b*-value between 0.5 and 1.5. However, the average *b*-value is accepted close to 1.0. According to these results, the magnitude-frequency distribution of earthquake database for the Marmara region matches the G-R relationship and this relatively large *b*-value means that the study region has a high frequency of small or moderate events. Hence, this situation may be considered as the high heterogeneity and low stress distribution in the study areas. The fractal statistic of the seismicity in the Marmara region was given in Figure 7b. Calculation of the *Dc*-value of the earthquake epicenters was made by fitting a straight line to the correlation integral curve, $C(R)$, against the epicenter distance R (km), in other words, log $C(r)$ versus log r. *Dc*-value was calculated as 1.57±0.03 for the 18,662 epicenter distributions with a 95% confidence limit by using linear regression. This log-log correlation function shows a noticeable linear interval and scale invariance in the cumulative statistic between 5.03 and 87.64 km. As shown in Figure 7b, the standard deviation was also computed within these distances and given on the figure. As mentioned above, earthquake distributions are related to the fractal dimension and therefore, they match the fractal statistics. Also, the fractal dimension is used as a quantitative measure of heterogeneity degrees in fault geometry. If there is increasing complexity in the active fault system with higher *Dc*-value and smaller b-value, the stress release occurs on fault planes of the smaller surface area [2]. Also, the larger *Dc*-value is sensitive to heterogeneity in magnitude distribution. *Dc*-value estimated as 1.57±0.03 suggests that seismicity is more clustered at larger scales or (in smaller areas) and this relatively large *Dc*-value may be a dominant structural characteristic for the study area. Since *Dc*-value is larger than 1.5, it can imply that Marmara seismicity is homogeneously distributed. Also, the seismic heterogeneity degree can be analyzed

quantitatively with the fractal dimension, and the heterogeneity of stress field controls the region [2], [17]. Hence, it can be obtained a non-heterogeneous stress distribution in the Marmara region. Thus, it can statistically be described and characterized by the regional distributions of earthquake epicenters and their fracture systems with fractal dimension.

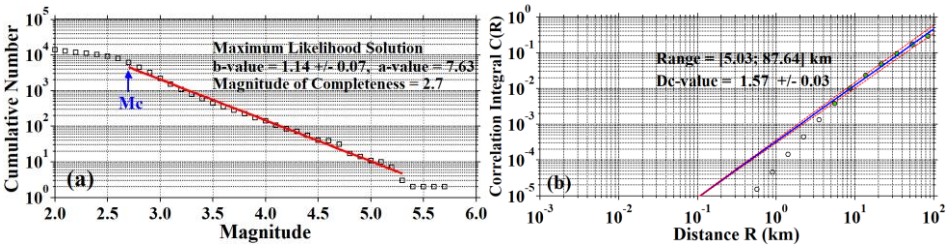

Figure 7. (a) Gutenberg-Richter, *b*-value, of magnitude-frequency distribution and (b) Fractal dimension, *Dc*-value, for the seismicity in Marmara region at the beginning of 2020. The slope of the blue line corresponds to *Dc*-value and red lines indicate the standard error.

One of the most critical steps in the description of earthquake behaviors is to evaluate the annual probabilities and recurrence times of the strong/large earthquake magnitudes. For this reason, this study includes these types of analyses and the results of the annual probabilities and recurrence times for different magnitude levels were plotted in Figure 8. Annual probabilities of the earthquake occurrences show relatively high values changing between 1 and 90 for the earthquake magnitudes with $3.0 \leq M_L < 4.2$, and the values smaller than 1 for the magnitude levels with $4.2 \leq M_L$ (Figure 8a). Recurrence times of the different magnitude levels were also plotted in Figure 8b. Recurrence times smaller than 1.0 year were observed for the magnitude levels between 2.5 and 4.2. Average recurrence times changing between 1 and 10 years were calculated for the earthquakes of $4.2 \leq M_L < 4.8$, whereas the recurrence times varying from 10 to 20 years were calculated for the earthquake magnitudes with $4.8 \leq M_L \leq 5.0$. In addition, recurrence times between 20 and 50 years can be estimated for the earthquakes with $5.0 < M_L \leq 5.2$, while the recurrence times greater than 50 years (between 50 and 300 years) can be expected for the earthquakes with $5.3 < M_L$ (Figure 8b). As mentioned above, a few strong/large earthquakes occurred in Marmara region in recent years: Saros Gulf, November 3, 2010 (*Ms*5.3), Marmara Sea, June 7, 2012 (*Ms*5.1), Gökçeada-Çanakkale, July 30, 2013 (*Ms*5.3) and Silivri-İstanbul, September 26, 2019 (*Ms*5.7) earthquakes. These results suggest that earthquakes with 3.0-4.2 magnitude sizes are more likely than those of the other occurrences, and a strong/large earthquake $5.0 \leq M_L$ can be expected in every 20 years. Therefore, these results show an existing seismic potential in and around the Marmara region.

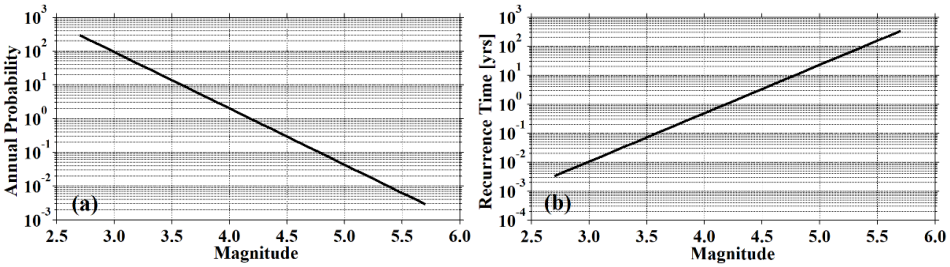

Figure 8. (a) Annual probabilities and (b) Recurrence times for different magnitude levels.

The details of $5.0 \leq M_L$ earthquakes in and around the Marmara region were given in Table 1. Also, temporal *b*-value change for the earthquake occurrences was plotted in Figure 9. In order to observe the variations in *b*-value as a function of time, a moving window technique and the maximum likelihood method were used. Temporal *b*-value estimation was made by a sample size of 350 earthquakes. The *b*-value variations were observed in a wide range from 0.6 to 2.0 and show some remarkable increases and decreases in about 20 years. Arrows in Figure 9 indicate the clear decreases in *b*-value before the occurrences of some strong/large earthquakes. As seen in Figure 9, the *b*-value shows great decreases before the occurrences of July 6, 2003 Saros Gulf and July 30, 2013 Kaleköy-Gökçeada earthquakes and clear increases after these earthquakes. These types of behaviors can also be clearly seen before the other earthquake occurrences given in Table 1. One can conclude from Figure 9 that these great and sudden decreases in *b*-value are related to the occurrence times of the main shocks, whereas the rapid increases are observed after the main shock occurrences. There are several factors causing perturbations in normal *b*-value. The applied shear stress may increase after the main shocks, which would be related to small *b*-values. Therefore, one can interpret that decreasing anomalies in *b*-value as a function of time before the occurrence times of the main shocks may be due to a stepwise increase (less or more) in the stress condition. Also, the relative numbers of small and large earthquakes before the occurrence of main shock may be related to the less or more decreases in *b*-value in different years. Therefore, observation of temporal *b*-value may have a statistical significance for the estimation of the next earthquakes in the Marmara region.

Table 1. Details of the strong/large earthquakes occurred in the Marmara region and its vicinity from 2000 to 2020.

Year	Month	Day	Origin Time	Latitude	Longitude	Depth (km)	Magnitude (M_L)	Environment
2000	08	23	13:41	40.71	30.75	9.0	5.0	Akyazı-Hendek
2003	07	06	19:10	40.39	26.19	12.0	5.7	Saros Gulf
2004	06	15	12:02	40.45	25.76	8.0	5.1	Saros Gulf
2006	10	20	18:15	40.26	27.98	10.9	5.2	Kuş Lake
2006	10	24	14:00	40.42	28.99	12.5	5.2	Gemlik Gulf
2008	12	28	22:58	40.41	25.81	8.8	5.2	Aegean Sea
2011	07	25	17:57	40.81	27.74	17.0	5.2	Marmara Sea
2012	06	07	20:54	40.85	27.92	14.9	5.1	Marmara Ereğlisi
2013	07	30	05:33	40.31	25.81	13.2	5.3	Kaleköy-Gökçeada
2014	05	24	09:31	40.43	26.24	7.2	5.1	Saros Gulf
2019	09	26	13:59	40.88	28.21	12.3	5.7	Silivri-İstanbul

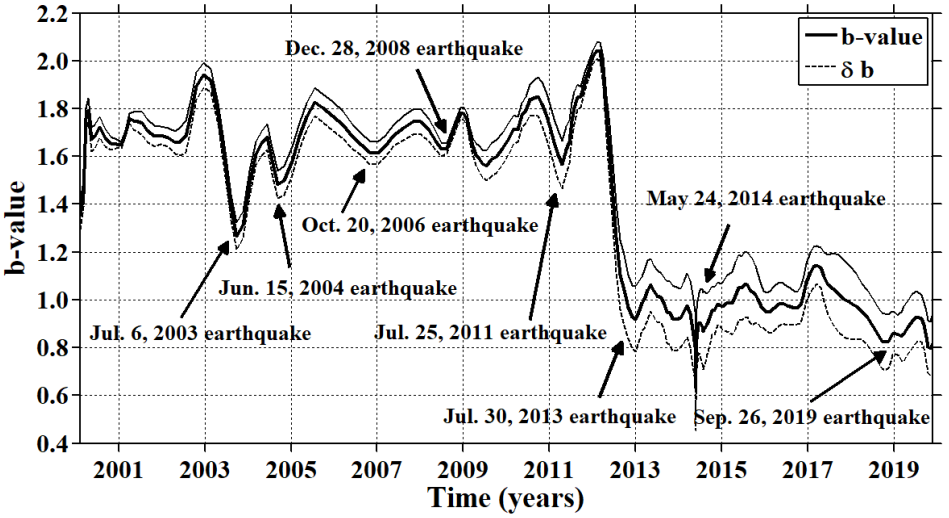

Figure 9. *b*-value changes as a function of time. Standard deviation of *b*-value (δ*b*) was also given. Arrows indicate the large decreases in *b*-value before the occurrences of strong/large earthquakes.

Regional changes of *b*-value at the beginning of 2020 were plotted by using a moving window approach in *ZMAP* with a sample of 500 events per window and a regional grid of 0.03°×0.03° in latitude and longitude. As seen in Figure 10, regional changes in the *b*-value are between 0.9 and 2.1. As mentioned above, the *b*-value of earthquake distributions is well represented by G-R relation with an average value of *b*=1.0 [35]. Depending on this statement, large *b*-values (>1.0) were observed across the study region. However, the regions with the smaller *b*-values (<1.0) were generally observed in the western part of the study region including the Aegean Sea. A larger proportion of small-magnitude earthquakes (Figure 3) generally occurred in the regions with higher *b*-values. However, the regions with lower *b*-values were observed in the areas in which large-magnitude earthquakes occur more often. In many parts of the Marmara region, large *b*-values (>1.0) were calculated and it can be attributed to the stress in these regions which is more easily decreased with a great number of small-magnitude earthquakes. It is suggested that smaller *b*-values make a sign of the higher stress release. Therefore, the smaller *b*-values may be an indication of low heterogeneity degree and high-strain [3] due to the active tectonics of the Marmara region. These small *b*-values can also be related to the stress to build up over time and to be released by events that are less frequent but large in magnitude [2]. As stated in many studies in literature, small *b*-values may show the regions in which the possible future earthquake will occur. Thus, a small *b*-value can be used to estimate the next earthquakes in these areas. However, in the regions with large *b*-values, this situation may be considered as evidence of low-stress relaxation by a great number of small earthquakes and thus, there may be a sizeable geological complexity in these regions. As a significant result, special attention should be paid to these parts of the Marmara region with an estimated small *b*-values.

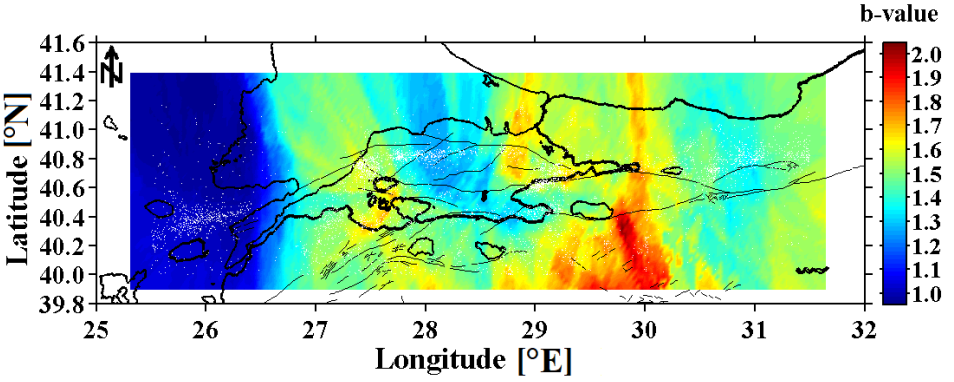

Figure 10. Regional changes of *b*-value at the beginning of 2020.

Seismicity rate changes for the Marmara region at the beginning of 2020 were mapped in Figure 11. As in the *b*-value map, a regional grid of 0.03° in latitude and longitude was used in order to image *Z*-value. The time window (Tw) was selected as 4.5 years to image the regional changes of Z-value. From the tests and assessments of the quiescence maps, we concluded that quiescence areas are better imaged for a time window of 4.5 years. As seen in Figure 11, there are several areas exhibiting precursory quiescence anomalies at the beginning of 2020. Anomaly regions displaying seismic quiescence at the beginning of 2020 are observed in the Aegean Sea, in and around SGF fault, the western part of Marmara Sea, in and around the MSF (including Erdek Gulf), throughout the GMF-İMF-GYF, in the EİDKF and its vicinity, in and around Sapanca Lake, and some parts in the Anatolian and European sides of İstanbul. Also, as seen in Figures 10 and 11, an evaluation of the regions with small *b*-value and large *Z*-value [3] may give useful keys to analyze the seismic potential in and around the Marmara region and thus, special emphasis needs to be paid to these anomaly regions.

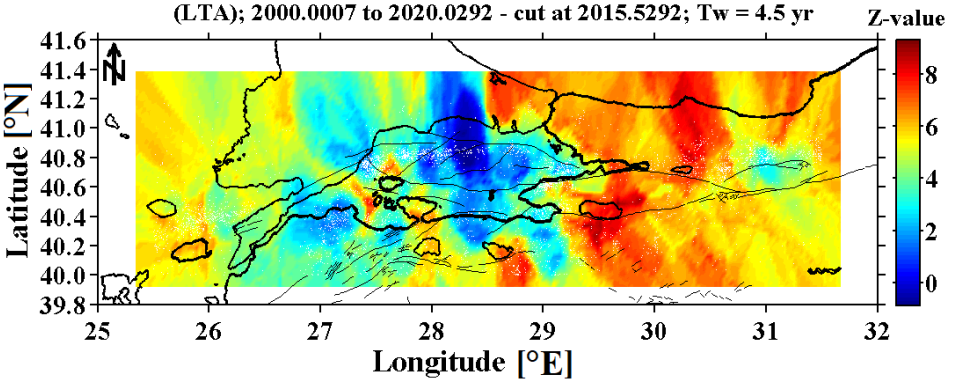

Figure 11. Regional changes of *Z*-value at the beginning of 2020.

In recent years, a number of studies have been achieved and different models have been used in order to describe the region-time-magnitude behaviors of the seismicity in different parts of Turkey, especially in the NAFZ [3], [5], [13], [44], [45], [46], [47], [48]. Pucci et al. [44] made a detailed comparison among the coseismic surface expression and the long term morphology and structural architecture of the Düzce fault zone in order to investigate the persistency or evolution

of the active fault formation at the surface. They stated that this analysis may supply some significant contributions to the estimation of the types for the next earthquake ruptures and segmentation models. Also, it is concluded that the local strain which affects the western part of the Düzce segment may act as a barrier and therefore, the rupture propagation from the İzmit to the Düzce fault segment may delay. Hence, they suggested that the eastern part of the Düzce segment may be a possible region for the future earthquake occurrence. Öztürk et al. [45] made a quantitative evaluation of seismic hazard parameters by using Gumbel's I asymptotic distribution for different parts of Turkey and its vicinity. They calculated the most possible magnitude, mean recurrence time and the earthquake occurrence possibility for the specific magnitude levels in a period of 10, 25, 50 and 100 years in different parts of Turkey including the NAFZ. The results of this study show that the mean recurrence times for $Ms \geq 6.5$ were estimated as 21.13±11.36 years for Düzce, Çankırı and Amasya regions, 37.15±18.81 years for İzmit, Gelibolu and Saros Gulf regions, 53.70±27.15 years for Çanakkale and its vicinity. When considered these results and some recent earthquakes such as March 18, 1953 Çanakkale, August 17, 1999 İzmit, November 12, 1999 Düzce which occurred in the NAFZ, they suggested that the average time of an earthquake occurrence with a magnitude $Ms \geq 6.5$ in these regions may be estimated as of 2020 and later. Öztürk [13] made a detailed assessment on the earthquake behaviors on different parts of the NAFZ by using *b*-value, *Dc*-value, *Z*-value and region-time-magnitude distribution of the earthquakes between1970 and 2010. They stated that some regions including Silivri, İzmit, Çanakkale, Düzce fault, Amasya, Erzincan, and Bingöl are important in terms of the future earthquake potential. 2010 Saros Gulf, 2011 Erzincan, 2013 Çanakkale and 2015 Bingöl earthquakes occurred within the regions estimated by Öztürk [13]. Karimi et al. [46] used integrated stress modeling and remote sensing techniques in order to describe the active fault geometries in the east of the Marmara Sea on the NAFZ. In relation to active fault geometries, they stated that obtained results can be expected to facilitate the long-term slip transfer. Also, they suggested that existing modeling will give useful information if the linking structures impede of facilitating the earthquake rupture propagation. Bohnhoff et al. [47] tried to determine the maximum earthquake magnitudes for the expected earthquake hazard throughout the different segments of the NAFZ. They found that the earthquakes between 7.8 and 8.0 are only observed along the older eastern segment of the NAFZ and this segment has longer coherent fault zones. Obtained results in Bohnhoff et al. [47] reveals that the maximum expected earthquake magnitude in the densely populated Marmara-İstanbul region would probably not exceed *M*7.5. Thus, these findings can help in the estimating hazard potential related to the different parts of the large transform faults. Öztürk [48] made a statistical study on the regional and temporal variations of seismicity in and around the NAFZ by using the *b*-value, *Dc*-value, *Z*-value and their correlations with each other. The regions exhibiting both the lowest *b*-value and the highest *Dc*-value with the high *Z*-value were given as the vicinity of Düzce fault and the Black Sea coast. Hence, it is stated that the decreases in *b*-value and the increases in *Dc*-value between 2012 and 2013 may be significant in terms of the future earthquake potential in the NAFZ and its vicinity. Also, seismic quiescence regions at the beginning of 2016 were observed in and around Enez, the north of Etili fault, Çanakkale and Edremit, Tekirdağ-Silivri and the Marmara Sea, the part of Black Sea and the vicinity of Yalova-İzmit, the northern part of Manyas fault, İznik-Gebze, Düzce fault, and the Black Sea coast. 2019 Silivri-İstanbul earthquake occurred within the areas predicted by Öztürk [48]. Thus, Öztürk [48] suggested that the combination of these seismicity parameters may provide preliminary and significant evidence in order to estimate the future earthquake occurrences in and around the NAFZ.

NAFZ was struck with large earthquakes in recent years as given in Table 1. Therefore, estimation of the next large earthquake in the Marmara region would be useful. When considering the former references and the proposed study, it can be seen that there is a potential for future earthquake occurrences in all different parts of the NAFZ. Therefore, a comparison of the anomaly regions of the *b*-value, *Dc*-value, *Z*-value which currently calculated in this study with

different geophysical parameters, especially stress distribution, will make significant contributions. In this point, a correlation and combined interpretation between these seismotectonic parameters may supply preliminary and significant information of seismic hazard for strong/large earthquake occurrences in the Marmara region of Turkey at the beginning of 2020.

5. CONCLUSIONS

A detailed statistical study on the region-time behaviors of the recent seismic activity in the Marmara region of Turkey at the beginning of 2020 was achieved. For this purpose, the most best known and the most frequently used hazard parameters such as *Mc*-value, *b*-value, *Dc*-value, *Z*-value, annual probability and recurrence time of earthquakes were preferred. A homogeneous catalog including 18,662 earthquakes with $0.4 \leq M_L \leq 5.7$ for shallow events between January 1, 2000 and January 21, 2020 was used and region-time behaviors of the earthquakes were mapped at the beginning of 2020. Reasenberg's algorithm was preferred to remove the dependent earthquakes from the catalog. *Mc*-value was calculated as 2.7. After declustering process and separating the earthquakes smaller than *Mc*-value, about 71.49% of total events was eliminated from the catalog and only 5320 earthquakes were used to map the regional distributions of seismicity parameters. Detailed region-time analyses suggest that the Marmara region has an intermediate/long terms seismic hazard in comparison to occurrences of strong/large earthquakes in the short term. According to the annual probability and recurrence time, the Marmara region has an intermediate/long terms hazard for the occurrence of strong/large earthquakes with $5.0 \leq M_L$. Also, the regions where anomalies were observed in the Marmara region must be carefully examined in terms of earthquake hazard and we recommend that earthquake activity should be monitored by locally dense arrays and must be evaluated with different geophysical parameters. As an important result, the anomaly regions showing small *b*-value and high *Z*-value with small recurrence times may be interpreted as the possible locations of the future strong/large earthquakes in the Marmara region.

Acknowledgment

We would like to thank to Prof. Dr. Stefan Wiemer for providing *ZMAP* software and the anonymous reviewers for their useful and constructive suggestions in improving this paper. We also grateful to KOERI and AFAD for providing the earthquake database.

REFERENCES

[1] S. Wiemer and M. Wyss, "Minimum magnitude of completeness in earthquake catalogs: Examples from Alaska, the Western United States, and Japan," *BSSA*, vol. 90, no. 3, pp. 859-869, 2000.

[2] A. O. Öncel and T. H. Wilson, "Space-time correlations of ceismotectonic parameters and examples from Japan and Turkey preceding the İzmit earthquake," *BSSA*, vol. 92, no. 1, pp. 339-350, 2002.

[3] O. Polat, E. Gok and D. Yılmaz, "Earthquake hazard of the Aegean extension region (west Turkey)," *Turkish J. Earth Sci.*, vol. 17, no. 3, pp. 593-614, 2008.

[4] S. Roy, U. Ghosh, S. Hazra and J. R. Kayal, "Fractal dimension and b-value mapping in the Andaman-Sumatra subduction zone," *Nat. Hazards*, vol. 57, pp. 27-37, 2011.

[5] S. Öztürk, "A statistical assessment of current seismic quiescence along the North Anatolian Fault Zone: Earthquake precursors," *Austrian J. Earth Sci*., vol. 106, no. 2, pp. 4-17, 2013.

[6] C. Raub, P. Martínez-Garzón, G. Kwiatek, M. Bohnhoff and G. Dresen, "Variations of seismic b-value at different stages of the seismic cycle along the North Anatolian Fault Zone in northwestern Turkey," *Tectonophysics*, vol. 712-713, pp. 232-248, 2017.

[7] C. Ozer, M. Ozyazicioglu, E. Gok and O. Polat, "Imaging the crustal structure throughout the East Anatolian Fault Zone, Turkey, by local earthquake tomography," *Pure Appl. Geophys.*, vol. 176, no. 6, 2235-2261, 2019.

[8] S. Uner, E. Ozsayin and A. S. Selcuk, "Seismites as an indicator for determination of earthquake recurrence interval: A case study from Erciş Fault (Eastern Anatolia-Turkey)," *Tectonophysics*, vol. 766, pp. 167-178, 2019.

[9] S. Öztürk, "A study on the variations of recent seismicity in and around the Central Anatolian region of Turkey," *Physics of the Earth and Planetary Interiors*, vol. 301, no. 106453, pp. 1-10, 2020.

[10] R. Gutenberg and C. F. Richter, "Frequency of earthquakes in California," *BSSA*, vol. 34, no. 4, pp. 185-188, 1944.

[11] C. H. Scholz, "The frequency-magnitude relation of microfracturing in rock and its relation to earthquakes," *BSSA*, vol. 58, pp. 399-415, 1968.

[12] B. Enescu and K. Ito, "Spatial analysis of the frequency-magnitude distribution and decay rate of aftershock activity of the 2000 Western Tottori earthquake," *Earth Planets Space*, vol. 54, pp. 847–859, 2002.

[13] S. Öztürk, "Characteristics of seismic activity in the western, central and eastern parts of the North Anatolian Fault Zone, Turkey: Temporal and spatial analysis," *Acta Geoph.*, vol. 59, no.2, pp. 209-238, 2011.

[14] S. Öztürk, "A study on the correlations between seismotectonic b-value and Dc-value, and seismic quiescence Z-value in the Western Anatolian region of Turkey," *Austrian J. Earth Sci.*, vol. 108, no. 2, pp. 172-184, 2015.

[15] K. Chiba, "Spatial and temporal distributions of b-values related to long-term slow-slip and low-frequency earthquakes in the Bungo Channel and Hyuga-nada regions, Japan," *Tectonophysics*, vol. 757, pp. 1-9, 2019.

[16] C. Goltz, "Fractal and chaotic properties of earthquakes," (Lecture Notes in Earth Sciences, 77) Springer-Verlag, 178 pp, 1998.

[17] A. O. Öncel and T. H. Wilson, "Correlation of seismotectonic variables and GPS strain-measurements in western Turkey," *J. Geophys. Res*., vol. 109(B11), no. B11306, 2004.

[18] S. Pailoplee and M. Choowong, "Earthquake frequency-magnitude distribution and fractal dimension in mainland Southeast Asia," *Earth Planets Space*, vol. 66, no. 8, pp. 1-10, 2014.

[19] S. Öztürk, "Earthquake hazard potential in the Eastern Anatolian part of Turkey: seismotectonic *b* and *Dc*-values, and precursory quiescence *Z*-value," *Frontiers of Earth Sci.*, vol. 12, no. 1, pp. 215-236, 2018.

[20] L. Telesca and Ch-ch. Chen, "Fractal and spectral investigation of the shallow seismicity in Taiwan," *J. Asian Earth Sci*., vol. 174, pp. 1-10, 2019.

[21] M. Wyss and A. H. Martirosyan, "Seismic quiescence before the M7, 1988, Spitak earthquake, Armenia," *Geophys. J. Int*., vol. 134, no. 2, pp. 329-340, 1998.

[22] M. Wyss and R. E. Habermann, "Precursory seismic quiescence," *Pure Appl. Geophys*., vol. 126, no. 2-4, pp. 319-332, 1988.

[23] W. J. Arabasz and M. Wyss, "Significant precursory seismic quiescences in the extensional Wasatch front region Utah," *EOS Trans. AGU* 77, F455, 1996.

[24] R. Console, C. Montuori and M. Murru, "Statistical assessment of seismicity patterns in Italy: Are they precursors of subsequent events?," *J. Seismol.*, vol. 4, pp. 435-449, 2000.

[25] K. Katsumata, "Precursory seismic quiescence before the Mw=8.3 Tokachi-oki, Japan, earthquake on 26 September 2003 revealed by a re-examined earthquake catalog," *J. Geophys. Res*., vol. 116, no. B10307, 2011.

[26] S. Öztürk, "Space-time assessing of the earthquake potential in recent years in the Eastern Anatolia region of Turkey," *Earth Sci. Res. J.*, vol. 21, no. 2, pp. 67-75, 2017.

[27] S. Gentili, A. Peresan, M. Talebi, M. Zare and R. D. Giovambattista, "A seismic quiescence before the 2017 Mw 7.3 Sarpol Zahab (Iran) earthquake: Detection and analysis by improved RTL method," *Phys. Earth Planet. Inter*., vol. 290, pp. 10-19, 2019.

[28] E. Bozkurt, "Neotectonics of Turkey – a synthesis," *Geodin. Acta*, vol. 14, no. 1-3, pp. 3-30, 2001.

[29] R. E. Reilinger, S. C. McClusky, M. B. Oral, W. King and M. N. Toksöz, "Global Positioning System measurements of present-day crustal movements in the Arabian-Africa-Eurasia plate collision zone," *J. Geoph. Res.*, vol. 102, pp. 9983-9999, 1997.

[30] F. Şaroğlu, Ö. Emre and İ. Kuşcu, "Active fault map of Turkey," *General Directorate of Mineral Research and Exploration*, Ankara, Turkey, 1992.

[31] R. Demirtaş and R. Yılmaz, "Türkiye'nin sismotektonigi; Sismisitedeki uzun süreli değişim ve güncel sismisiteyi esas alarak deprem tahminine bir yaklaşım," T.C. Bayındırlık ve İskan Bakanlığı Yayını, 91 s., Ankara, 1996.

[32] Ö. Emre, T. Y. Duman, S. Özalp, F. Şaroğlu, Ş. Olgun, H. Elmacı and T. Çan, "Active fault database of Turkey," *Bull. Earthquake Eng*., vol. 16, pp. 3229-3275, 2018.

[33] D. Kalafat, "Statistical Evaluation of Turkey Earthquake Data (1900-2015): A Case study," *Eastern Anatolian Journal of Science*, vol. 2, pp. 14-36, 2016.

[34] T. Utsu, "Aftershock and Earthquake Statistic (III): Analyses of the Distribution of Earthquakes in Magnitude, Time and Space with Special Consideration to Clustering Characteristics of Earthquake Occurrence (1)", *J. of Faculty of Sci., Hokkaido Univ.*, Series VII (Geophysics) vol. 3, no. 5, pp. 379-441, 1971.

[35] C. Frohlich and S. Davis, "Teleseismic b-values: Or, much ado about 1.0," *J. Geoph. Res.*, vol. 98, no. B1, pp. 631-644, 1993.

[36] K. Mogi, "Magnitude-frequency relation for elastic shocks accompanying fractures of various materials and some related problems in earthquakes," *Bull. Earthquake Res. Inst*., *Tokyo Univ*., vol. 40, pp. 831-853, 1962.

[37] R. Grassberger and I. Procaccia, "Measuring the Strangeness of Strange Attractors," *Physica*, vol. 9, no. 1-2, pp. 189-208, 1983.

[38] M. Wyss and R. E. Habermann, "Precursory seismic quiescence," *PAGEOPH*, vol. 126, no. 2-4, pp. 319-332, 1988.

[39] S. Wiemer and M. Wyss, "Seismic quiescence before the Landers (M=7.5) and Big Bear (6.5) 1992 earthquakes," *BSSA*, vol. 84, no. 3, pp. 900-916, 1994.

[40] S. Wimer, "A software package to analyze seismicity: ZMAP," *Seismol. Res. Lett.*, vol. 72, no. 2, pp. 373-382, 2001.

[41] P. A. Reasenberg, "Second-order moment of central California seismicity, 1969-1982," *J. Geoph. Res.*, vol. 90, no. B7, pp. 5479-5495, 1985.

[42] K. Katsumata and M. Kasahara, "Precursory seismic quiescence before the 1994 Kurile Earthquake (Mw=8.3) revealed by three independent seismic catalogs," *PAGEOPH*, vol. 155, pp. 43-470, 1999.

[43] J. D. R. Joseph, K. B. Rao and M. B. Anoop, "A study on clustered and de-clustered world-wide earthquake data using G-R recurrence law," *International Journal of Earth Sciences and Engineering*, vol. 4, pp. 178-182, 2011.

[44] S. Pucci, D. Pantosti, M. R. Barchi and N. Palyvos, "A complex seismogenic shear zone: The Düzce segment of North Anatolian Fault (Turkey)," *Earth and Planetary Science Letters*, vol. 262, pp. 185-203, 2007.

[45] S. Öztürk, Y. Bayrak, H, Çınar, G.Ch. Koravos and T. M. Tsapanos, "A quantitative appraisal of earthquake hazard parameters computed from Gumbel I method for different regions in and around Turkey, *Natural Hazards*, vol. 47, pp. 471-495, 2008.

[46] B. Karimi, N. McQuarrie, J-S. Lin and W. Harbert, "Determining the geometry of the North Anatolian Fault East of the Marmara Sea through integrated stress modeling and remote sensing techniques," *Tectonophysics*, vol. 623, pp. 14-22, 2014.

[47] M. Bohnhoff, P. Martínez-Garzón, F. Bulut, E. Stierle and Y. Ben-Zion, "Maximum earthquake magnitudes along different sections of the North Anatolian fault zone," *Tectonophysics*, vol. 674, pp. 147-165, 2016.

[48] S. Öztürk, "Regional and temporal analyses of the current earthquake activity in and around the North Anatolian Fault Zone," *Bulletin for Earth Sciences*, vol. 38, no. 2, pp. 193-228, 2017.

[49] URL-1. http://www.koeri.boun.edu.tr/sismo/2/category/basinbultenleri/, 30/03/2020.